Nonsmooth contact dynamics for the numerical simulation of collisions in musical string instruments

Clara Issanchou,[1,a)] Vincent Acary,[2] Franck Pérignon,[2] Cyril Touzé,[3,b)] and Jean-Loïc Le Carrou[1]

[1]*Sorbonne Université, Centre National de la Recherche Scientifique, équipe Lutheries-Acoustique-Musique, Institut Jean Le Rond d'Alembert, 4 place Jussieu, 75252 Paris Cedex 05, France,*
[2]*Université Grenoble Alpes, Centre National de la Recherche Scientifique, Inria, Institut Polytechnique de Grenoble, Laboratoire Jean Kuntzmann, 655, Avenue de l'Europe, 38334 Saint Ismier Cedex, France*
[3]*Institute of Mechanical Sciences and Industrial Applications, École Nationale Supérieure de Techniques Avancées ParisTech, Centre National de la Recherche Scientifique, Université Paris Saclay, 828 Boulevard des Maréchaux, 91762 Palaiseau Cedex, France*

Collisions in musical string instruments play a fundamental role in explaining the sound production in various instruments such as sitars, tanpuras, and electric basses. Contacts occurring during the vibration provide a nonlinear effect which shapes a specific tone due to energy transfers and enriches the hearing experience. As such, they must be carefully simulated for the purpose of physically based sound synthesis. Most of the numerical methods presented in the literature rely on a compliant modeling of the contact force between the string and the obstacle. In this contribution, numerical methods from nonsmooth contact dynamics are used to integrate the problem in time. A Moreau-Jean time-stepping scheme is combined with an exact scheme for phases with no contact, thus controlling the numerical dispersion. Results for a two-point bridge mimicking a tanpura and an electric bass are presented, showing the ability of the method to deal efficiently with such problems while invoking, as compared to a compliant approach, less modelling parameters, and a reduced computational burden. © 2018 Acoustical Society of America. https://doi.org/10.1121/1.5039740

[TRM]   Pages: 3195–3205

I. INTRODUCTION

Collisions are of prime importance in musical acoustics for explaining the particular timbre of a number of instruments ranging from strings (a typical example being that of Indian instruments such as sitar, tanpura, and veena) to drums (e.g., snare drum) (Bilbao, 2012; Fletcher and Rossing, 1998; Raman, 1921). In these examples, the role of contacts is to alter the frequency content due to a nonlinear, nonsmooth interaction that generates high frequencies and contributes to enrich the hearing experience. This effect is particularly prominent in the case of the sitar, where a curved bridge contributes to significantly modify the frequency content of the string vibration (e.g., Bilbao *et al.*, 2015; Mandal and Wahi, 2015; Siddiq, 2012; Vyasarayani *et al.*, 2009), and in the case of the tanpura and its particular bridge (Chatziioannou and van Walstijn, 2015; Issanchou *et al.*, 2017; Valette *et al.*, 1991). Other examples that attracted interest in the recent years concern the case of string/frets interactions (e.g., guitar or electric bass) (Bilbao and Torin, 2015; Issanchou *et al.*, 2018; Trautmann and Rabenstein, 2004) and snare drum where metal wires are in contact with a vibrating membrane (Bilbao, 2012; Bilbao *et al.*, 2015).

Earlier studies on vibrating strings with contacts derive a number of analytical results, mostly in the 1980s (Amerio, 1978; Cabannes, 1987; Citrini, 1991; Schatzman, 1980). To overcome the limitations of these approaches, where the string needs to be perfect without stiffness, thus discarding the dispersive effect which has been shown to be of prime importance in the case of the sitar and tanpura (Chatziioannou and van Walstijn, 2015; Issanchou *et al.*, 2017; Siddiq, 2012), recent research efforts concentrate toward the development of efficient, robust, and accurate numerical methods in order to simulate musical strings encountering an obstacle during their vibration. Most of the methods presented recently use a regularisation in order to numerically treat the contact force, see, e.g., the energy-conserving schemes proposed by Bilbao and co-workers (Bilbao *et al.*, 2015; Desvages and Bilbao, 2015; Ducceschi *et al.*, 2016) and by van Walstijn and co-workers (Chatziioannou and van Walstijn, 2015; van Walstijn and Bridges, 2016; van Walstijn *et al.*, 2016), the modal approach proposed in Issanchou *et al.* (2017), or the approach followed in Inácio *et al.* (2006) to model the interaction between a *puja* (exciting stick) and a Tibetan bowl. In all of these studies, the contact force is modeled using a power-law method with two parameters defining the stiffness of the repelling force, thus allowing one to cover a wide

range of contact laws, from soft collisions, e.g., contact between felt and hammer in piano (Boutillon, 1988), between mallet and membrane in a kettledrum (Rhaouti *et al.*, 1999), or between finger and fretboard (Bilbao and Torin, 2015), to hard contacts. In this article, we will name the methods using a regularisation to express the repelling force a "compliant approach." In this framework, power laws are often used but other functions may also be selected. Also, the parameters defining the contact force may have a physical basis, see Goldsmith (2001) for some examples. On the other hand, *ad hoc* values may be used as numerical free parameters, so that a penalty approach is at hand.

On the other hand, a large body of research has been dedicated to the development of nonsmooth numerical methods in order to deal efficiently with numerical challenges posed by contact and friction forces. These methods rely on specific assumptions (e.g., no interpenetration is allowed between the contacting bodies) and use mathematical tools from the measure theory, differential inclusions, and complementarity systems. The first developments have been pioneered by Jean and Moreau (see, e.g., Jean, 1999; Jean and Moreau, 1987), continued by numerous investigations (Doyen *et al.*, 2011; Janin and Lamarque, 2001; Paoli and Schatzman, 2002), and are now summarized in reference books (Acary and Brogliato, 2008; Studer, 2009). Nonsmooth methods have been successfully applied in a variety of contexts ranging from granular media (Renouf *et al.*, 2004), geomaterials (Jean, 1995), multibody dynamics (Chen *et al.*, 2013) to realistic simulations of hair motions and living systems (Acary *et al.*, 2014; Bertails-Descoubes *et al.*, 2011). In the field of vibration, the method has been applied to rotor/casing contacts in Meingast *et al.* (2014) as well as to string vibrations in Ahn (2007), where the study was, however, limited to the case of a perfect string without stiffness and a frictionless contact. In the area of musical acoustics, the action of a grand piano has been recently simulated efficiently by using a nonsmooth approach (Thorin *et al.*, 2017).

As remarked by a number of investigators, numerical integration for contact dynamics is generally time-consuming due to the high-frequency content generated (Doyen *et al.*, 2011; Issanchou *et al.*, 2017), leading to the consideration of very small time steps in order to achieve convergence. In this context, nonsmooth numerical methods, such as avoiding the costly step of finding the zeros of a non-linear function with a Newton-Raphson approach and using efficient numerical methods to solve a linear complementarity problem, should decrease the computational burden (Acary and Brogliato, 2008). From the modeling point of view, nonsmooth methods are particularly appealing when one only needs an efficient numerical method to repel a vibrating structure from an obstacle with a simple representation of the dissipation phenomena at contact. As such, nonsmooth methods describe the contact law with a single parameter, the coefficient of restitution, instead of the two parameters used in the power-law approach as done in, e.g., Bilbao *et al.* (2015), Chatziioannou and van Walstijn (2015), and Issanchou *et al.* (2017) in the conservative case, and additional parameters to model the dissipation following a

Hunt and Crossley approach. Let us note that it is also difficult with the power-law approach to obtain large dissipation rates at contact. For this purpose, more complicated compliant models must be introduced including plasticity effects (Nguyen and Brogliato, 2014). Less modelling parameters could be seen as an advantage, but also as a drawback if one prefers to have more degrees of freedom in order to represent different contact laws with a large variety of stiffness and/or damping to account for a physical reality having perceptual effects. A typical example is that of the guitar where very different parameters are used for the string/fret and finger/fingerboard collisions (Bilbao and Torin, 2015). Note, however, that nonsmooth methods can also be conjugated with a material description of a soft structure including nonlinear stiffness and damping to account for these effects and tune them at ease, see, e.g., the recent modeling of felt in piano action proposed in Thorin *et al.* (2017).

In this contribution, a nonsmooth numerical approach based on a Moreau-Jean time-stepping scheme is adapted to the case of a string vibrating against a stiff obstacle with hard contacts, for the specific purpose of musical acoustics. The examples have been purposely chosen to restrict our discussion to hard contacts where the nonsmooth method should be an interesting alternative to compliant approaches. Standard nonsmooth methods are known to produce numerical dispersion (Yoong *et al.*, 2017), which is a specific issue in the field of musical acoustics. During non-contacting phases, an exact scheme, introduced in Bilbao (2009) and used for compliant contact approaches in Issanchou *et al.* (2017) and van Walstijn and Bridges (2016), is considered in order to ensure a numerical integration method with controlled dispersion. The efficiency of the scheme is demonstrated on two examples which are compared either to a compliant approach or to experimental results. First, the case of a two-point bridge mimicking a tanpura is shown. Results are then extended to a fretted electric bass having at most 20 contact points. The accuracy of the two different modeling options (nonsmooth vs compliant approach) are discussed and the computational burdens of these methods are compared.

II. MODEL

A. Vibrating string against a unilateral obstacle

We consider a stiff string of length L (m), mass per unit length μ (kg m^{-1}), and tension T (N). Its Young's modulus E (Pa) and moment of inertia I define its stiffness. The string vibrates against a unilateral obstacle, the profile of which is described by $g(x)$ (see Fig. 1). Equation (1) describes the displacement of the string along (Oz),
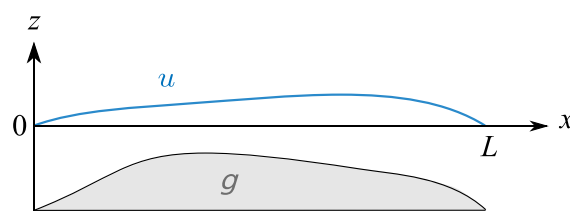

FIG. 1. (Color online) Scheme of a string vibrating against a unilateral obstacle.

$$\mu u_{tt} - T u_{xx} + EI u_{xxxx} = f(x,t), \tag{1}$$

where the subscript t (respectively, x) refers to a partial derivative with respect to time (respectively, space). The right-hand side $f(x, t)$ refers to the contact force per unit length.

The string is simply supported at its endpoints, so that $\forall t \in \mathbb{R}^+ : u(0,t) = u(L,t) = u_{xx}(0,t) = u_{xx}(L,t) = 0$. In order to achieve a fine representation of eigenfrequencies and damping parameters, we employ the following modal description of the string:

$$u(x,t) = \sum_{j=1}^{N_m} q_j(t)\phi_j(x), \tag{2}$$

where $\phi_j(x) = \sqrt{2/L}\sin(j\pi x/L)$ and q_j is the jth modal amplitude.

Inserting the modal expansion (2) into the equation of motion (1), multiplying by another mode shape and integrating over the string length, and then adding losses to the final modal equations, one obtains

$$\mu(\ddot{\mathbf{q}} + \Omega^2\mathbf{q} + 2\Upsilon\dot{\mathbf{q}}) = \mathbf{F}, \tag{3}$$

where $\mathbf{q} = [q_1, q_2, ..., q_{N_m}]^T$ is the vector of unknown modal amplitudes. Ω and Υ are diagonal matrices such that Ω contains radian frequencies $\Omega_{jj} = \omega_j = 2\pi\nu_j$, ν_j being the jth eigenfrequency, and Υ contains damping coefficients $\Upsilon_{jj} = \sigma_j$. These quantities follow the model presented in Issanchou *et al.* (2017), Issanchou *et al.* (2018), Paté *et al.* (2014), and Valette and Cuesta (1993). We briefly recall the expression of eigenfrequencies and damping parameters in the Appendix. The vector $\mathbf{F}$ contains modal forces and represents the projection of the contact force onto mode shapes, its entries read $F_p = \int_0^l f(x,t)\phi_p(x)\mathrm{d}x$, for $p \in \{1, ..., N_m\}$.

B. Contact force

We choose to model the contact condition by a unilateral constraint in order to avoid the interpenetration of the solids. Defining $\eta(x,t) = u(x,t) - g(x)$ as the distance between the string and the obstacle, this constraint is given by

$$\eta(x,t) \geq 0, \forall t \in \mathbb{R}^+. \tag{4}$$

In order to satisfy Eq. (4), the reaction force introduced in Eq. (1) has to be positive and vanishes only if the constraint is not active (open contact). The complete model is the Signorini law which can be simply written with the following notation (Acary and Brogliato, 2008; Signorini, 1933):

$$0 \leq \eta(x,t) \perp f(x,t) \geq 0, \tag{5}$$

meaning that either $\eta(x,t) = 0$ and $f(x,t) \geq 0$, or $f(x,t) = 0$ and $\eta(x,t) \geq 0$.

Second order dynamics with unilateral constraints involves velocity jumps. The usual setting is to consider that the velocity map $t \mapsto u_t(x,t)$ is a right continuous function,

i.e., $u_t^+(x,t) = u_t(x,t)$, and of bounded variation. The notation $u_t^+(x,t)$ [respectively, $u_t^-(x,t)$] stands for the right limit (respectively, the left limit) of $t \mapsto u_t(x,t)$ at time t, i.e., $u_t^+(x,t) = \lim_{\substack{s \to t \\ s > t}} u_t(x,s)$ (respectively, $u_t^-(x,t) = \lim_{\substack{s \to t \\ s < t}} u_t(x,s)$). Since the function is of bounded variation, these limits exist.

In order to define the solution, especially in a discrete (finite-dimensional) system, a condition on the velocity after an impact must be specified. To this purpose, we choose the Newton impact law (Acary, 2016)

$$\dot{\eta}^+(x,t) = -\varrho\dot{\eta}^-(x,t) \quad \text{if } \eta(x,t) = 0, \tag{6}$$

where the coefficient of restitution $\varrho \in [0, 1]$ defines the string behaviour at impact instants.

In the sequel, the Signorini law is formulated at the velocity level, which allows one to explicitly control contact losses taking into account the Signorini condition together with the impact law. Therefore, the contact law is written as

$$\begin{cases} 0 \leq \dot{\eta}^+(x,t) + \varrho\dot{\eta}^-(x,t) \perp f(x,t) \geq 0 & \text{if } \eta(x,t) = 0, \\ f(x,t) = 0 & \text{otherwise.} \end{cases} \tag{7}$$

The viability lemma of Moreau (1999) ensures that the condition at the velocity level (7) implies the condition at the position level (5) if the constraint (4) is satisfied at the initial time.

Since the system has some discontinuities in the velocity $\mathbf{w} = \dot{\mathbf{q}}$, the acceleration $\dot{\mathbf{w}}$ is not defined everywhere in the classical sense. A differential measure $\mathrm{d}\mathbf{w}$ is associated with the velocity $\mathbf{w}$ and plays the role of the acceleration. If we also assume that $\mathbf{w}$ is of special bounded variation (i.e., $\mathbf{w}$ may be decomposed into a sum of an absolutely continuous function and a jump function), the differential measure can be decomposed with respect to the Lebesgue measure $\mathrm{d}t$ as

$$\mathrm{d}\mathbf{w} = \ddot{\mathbf{q}}\mathrm{d}t + (\mathbf{w}^+ - \mathbf{w}^-)\mathrm{d}\tilde{\nu}, \tag{8}$$

where $\mathrm{d}\tilde{\nu}$ is a discrete measure of the form $\Sigma_i a_i\delta_{s_i}$ with given sequences $\{a_i\}$ and $\{s_i\}$ of real numbers. The notation δ_s refers to the Dirac measure supported at time s [see, e.g., Moreau (1988) for details on differential measures]. In other words, $\dot{\mathbf{w}}(t) = \ddot{\mathbf{q}}(t)$ almost everywhere and at impact instants t^* we have $\mathrm{d}\mathbf{w} = (\mathbf{w}^+ - \mathbf{w}^-)\delta_{t^*}$. Similarly, the reaction force in the modal space is defined by a vector measure

$$\mathrm{d}\mathbf{I} = \mathbf{F}\mathrm{d}t + \mathbf{P}\mathrm{d}\tilde{\nu}, \tag{9}$$

where the vector $\mathbf{F}$ corresponds to a modal continuous contact force and the vector $\mathbf{P}$ is a modal contact impulse corresponding to velocity jumps. In terms of differential measure, the modal equations read as

$$\mu(\mathrm{d}\mathbf{w} + \Omega^2\mathbf{q}\mathrm{d}t + 2\Upsilon\dot{\mathbf{q}}\mathrm{d}t) = \mathrm{d}\mathbf{I}. \tag{10}$$

By substituting Eqs. (8) and (9) in Eq. (10), we remark that Eq. (3) is satisfied $\mathrm{d}t$-almost everywhere. At the instants of discontinuities, we obtain the impact equation

J. Acoust. Soc. Am. **143** (5), May 2018

Issanchou *et al.* 3197

$$\mu(\mathbf{w}^+ - \mathbf{w}^-) = \mathbf{P}. \tag{11}$$

The contact condition at the velocity level is also reformulated in terms of measures as follows:

$$\begin{cases} 0 \le \dot\eta^+(x,t) + \varrho\dot\eta^-(x,t) \perp di \ge 0 & \text{if } \eta(x,t) = 0, \\ di = 0 & \text{otherwise,} \end{cases} \tag{12}$$

where di is the reaction force in the physical space. The relation between η, $\dot\eta$ and $\mathbf{q}$, $\dot{\mathbf{q}}$ is given by the relations between the quantities in the physical space and the modal space. Let us introduce the column vector $\phi(x)$ containing the N_m first string modes, defined by $\phi_j = \phi_j(x)$, $\forall j \in \{1, ..., N_m\}$. From Eq. (2), we get that $u(x,t) = \phi^T(x)\mathbf{q}(t)$ where $\mathbf{q} = [q_1(t), ..., q_{N_m}(t)]^T$ and therefore

$$\eta(x,t) = \phi^T(x)\mathbf{q}(t) - g(x) \quad \text{and} \quad \dot\eta(x,t) = \phi^T(x)\dot{\mathbf{q}}(t). \tag{13}$$

By duality, we also have

$$dI_j = \int_0^L \phi_j di dx. \tag{14}$$

Altogether, the dynamics is given by the following measure differential complementarity problem:

$$\dot{\mathbf{q}} = \mathbf{w}, \tag{15a}$$

$$\mu(d\mathbf{w} + \Omega^2 \mathbf{q}dt + 2\Upsilon\dot{\mathbf{q}}dt) = d\mathbf{I}, \tag{15b}$$

$$\mathbf{q}(0) = \mathbf{q}_0, \mathbf{w}(0) = \mathbf{w}_0, \tag{15c}$$

$$\eta = \phi^T\mathbf{q} - g, \tag{15d}$$

$$\dot\eta = \phi^T\dot{\mathbf{q}}, \tag{15e}$$

$$dI_j = \int_0^L \phi_j di dx, \tag{15f}$$

$$0 \le \dot\eta^+ + \varrho\dot\eta^- \perp di \ge 0 \quad \text{if } \eta \le 0. \tag{15g}$$

III. NUMERICAL METHOD

In this section, we present a discretisation of the problem presented in Sec. II, which is able to handle nonsmooth contacts. The distinctive feature of the proposed scheme is to combine an exact method for the linear (non-contacting) part of the equations of motion with a Moreau-Jean time-stepping approach to handle impulses and velocity jumps. The resulting scheme thus prevents dispersion when the string freely vibrates, which represents an improvement of already existing nonsmooth time-stepping methods.

In the rest of the paper, the variable t^n denotes the discrete time $t^n = n\Delta t$, where Δt is the time step. The spatial grid is defined by $x_i = i\Delta x$, $\forall i \in \{0, ..., N\}$, where $\Delta x = L/N$ is the spatial step. Due to selected boundary conditions, $u(x_0, t) = 0$ and $u(x_N, t) = 0$ $\forall t \in \mathbb{R}^+$, so only the interior points of the grid are considered.

As prescribed in a Moreau-Jean scheme, Eq. (15b) is integrated over $(t^n, t^{n+1}]$. One thus obtains

$$\mu(\mathbf{w}^+(t^{n+1}) - \mathbf{w}^+(t^n)) + \mu\Omega^2 \int_{t^n}^{t^{n+1}} \mathbf{q}dt + 2\mu\Upsilon \int_{t^n}^{t^{n+1}} \dot{\mathbf{q}}dt$$
$$= \int_{(t^n, t^{n+1}]} d\mathbf{I}. \tag{16}$$

The collision term on the right-hand side of Eq. (16) is treated with the Moreau-Jean scheme, leading to the following discrete approximation:

$$P_i^{n+1} \approx \int_{(t^n, t^{n+1}]} dI_i, \tag{17}$$

where $\mathbf{P}^{n+1} = [P_1^{n+1}, ..., P_{N-1}^{n+1}]^T$ is a contact impulse over the time interval, which will be defined later through a complementarity condition. The Moreau-Jean scheme is generally used with a θ-method to approximate the stiffness and damping terms in Eq. (16), as prescribed, for example, in Acary and Brogliato (2008), Jean (1999), Jean and Moreau (1987), and Moreau (1999). However, for mechanical vibratory systems expressed in the modal basis and with application to musical acoustics where the problem of numerical dispersion is particularly stringent, the exact scheme used in Bilbao (2009) and Issanchou et al. (2017) shall be considered in order to improve the discretisation of the stiffness and damping terms. Using the notations for discrete approximations, $w_i^n \approx w_i^+(t^n)$, and $q_i^n \approx q_i(t^n)$, it reads

$$\int_{t^n}^{t^{n+1}} q_i dt \approx \frac{\Delta t q_i^n}{1 + (1 - \gamma_i)\dfrac{\omega_i^2\Delta t^2}{2} + \sigma_i^*\Delta t}, \tag{18}$$

$$\int_{t^n}^{t^{n+1}} \sigma_i \dot{q}_i dt \approx \frac{\sigma_i^*\Delta t w_i^n}{1 + (1 - \gamma_i)\dfrac{\omega_i^2\Delta t^2}{2} + \sigma_i^*\Delta t}, \tag{19}$$

where the introduced terms γ_i and σ_i^* are such that

$$\gamma_i = \frac{2}{\omega_i^2\Delta t^2} - \frac{A_i}{1 + e_i - A_i}, \tag{20}$$

$$\sigma_i^* = \left(\frac{1}{\Delta t} + \frac{\omega_i^2\Delta t}{2} - \gamma_i\frac{\omega_i^2\Delta t}{2}\right)\frac{1 - e_i}{1 + e_i}, \tag{21}$$

with

$$A_i = e^{-\sigma_i\Delta t}(e^{\sqrt{\sigma_i^2 - \omega_i^2}\Delta t} + e^{-\sqrt{\sigma_i^2 - \omega_i^2}\Delta t}), \tag{22}$$

$$e_i = e^{-2\sigma_i\Delta t}. \tag{23}$$

Finally, one obtains the following time-stepping scheme from Eq. (16) for the update of the modal velocity vector using Eqs. (18) and (19):

$$w_i^{n+1} - w_i^n + \frac{\Delta t\omega_i^2}{1 + (1 - \gamma_i)\dfrac{\omega_i^2\Delta t^2}{2} + \sigma_i^*\Delta t}q_i^n$$
$$+ \frac{2\Delta t\sigma_i^*}{1 + (1 - \gamma_i)\dfrac{\omega_i^2\Delta t^2}{2} + \sigma_i^*\Delta t}w_i^n = \frac{1}{\mu}P_i^{n+1}. \tag{24}$$

In matrix form, it is written

$$\mathbf{w}^{n+1} - \mathbf{w}^n + \Delta t \mathbf{C} \mathbf{q}^n + \Delta t \check{\mathbf{C}} \mathbf{w}^n = \frac{1}{\mu} \mathbf{P}^{n+1}, \qquad (25)$$

where $\mathbf{C}$ and $\check{\mathbf{C}}$ are diagonal matrices with entries

$$C_{ii} = \frac{\omega_i^2}{1 + (1-\gamma_i)\frac{\omega_i^2 \Delta t^2}{2} + \sigma_i^* \Delta t},$$

$$\check{C}_{ii} = \frac{2\sigma_i^*}{1 + (1-\gamma_i)\frac{\omega_i^2 \Delta t^2}{2} + \sigma_i^* \Delta t}.$$

The update of the modal amplitudes is given by the discretisation of Eq. (15a) as

$$q_i^{n+1} = q_i^n + \Delta t w_i^{n+1}. \qquad (26)$$

We introduce a matrix $\mathbf{S}$ containing the N_m first string modes, defined by $S_{ij} = \phi_j(x_i)$, $\forall (i,j) \in \{1,...,N-1\} \times \{1,...,N_m\}$. Defining the physical discrete displacement vector $\mathbf{u} = [u(x_1,t), ..., u(x_{N-1},t)]^T$, one easily obtains the following relationship: $\mathbf{u} = \mathbf{S}\mathbf{q}$ (Issanchou *et al.*, 2017). Denoting the displacement of the string at contact points by $\mathbf{u}_c = \mathbf{S}_c \mathbf{q}$, its velocity by $\mathbf{v}_c = \mathbf{S}_c \mathbf{w}$ and introducing the velocity without contact $\mathbf{w}_{\text{free}}^{n+1}$ as

$$\mathbf{w}_{\text{free}}^{n+1} = \mathbf{w}^n - \Delta t \mathbf{C} \mathbf{q}^n - \Delta t \check{\mathbf{C}} \mathbf{w}^n, \qquad (27)$$

one obtains the following linear equation between $\mathbf{v}_c^{n+1}$ and $\mathbf{p}_c^{n+1}$, with $\mathbf{P}^n = \Delta x \mathbf{S}_c^T \mathbf{p}_c^n$:

$$\mathbf{v}_c^{n+1} = \mathbf{S}_c \mathbf{w}_{\text{free}}^{n+1} + \mathbf{W}_{cc} \mathbf{p}_c^{n+1}, \qquad (28)$$

where the Delassus' matrix $\mathbf{W}_{cc}$ is computed as

$$\mathbf{W}_{cc} = \frac{\Delta x}{\mu} \mathbf{S}_c \mathbf{S}_c^T. \qquad (29)$$

The complementarity condition (15g) is discretised in a fully implicit way as prescribed for the Moreau-Jean scheme. For a contact point indexed by c_i, one has to solve

$$\begin{cases} \mathbf{p}_{c_i}^{n+1} = 0 & \text{if } \boldsymbol{\eta}_{c_i}^n > 0, \\ 0 \leq \boldsymbol{v}_{c_i}^{n+1} + \varrho \boldsymbol{v}_{c_i}^n \perp \mathbf{p}_{c_i}^{n+1} \geq 0 & \text{if } \boldsymbol{\eta}_{c_i}^n \leq 0. \end{cases} \qquad (30)$$

Let us denote the index set of active contact points as Q_{te}^{-1}. The impulse $\mathbf{p}_{\bar{c}}^{n+1}$ is the solution of

$$\begin{cases} \mathbf{v}_{\bar{c}}^{n+1} = \mathbf{S}_{\bar{c}} \mathbf{w}_{\text{free}}^{n+1} + \mathbf{W}_{\bar{c}\bar{c}} \mathbf{p}_{\bar{c}}^{n+1}, \\ 0 \leq \boldsymbol{v}_{\bar{c}}^{n+1} + \varrho \boldsymbol{v}_{\bar{c}}^n \perp \mathbf{p}_{\bar{c}}^{n+1} \geq 0, \end{cases} \qquad (31)$$

which is a linear complementarity problem (LCP). A LCP consists in finding the vectors $\mathbf{z}, \boldsymbol{\lambda}$ such that

$$\begin{cases} \mathbf{z} = \mathbf{W}\boldsymbol{\lambda} + \mathbf{a}, \\ 0 \leq \mathbf{z} \perp \boldsymbol{\lambda} \geq 0 \end{cases} \qquad (32)$$

for some given matrix $\mathbf{W}$ and given vector $\mathbf{a}$. Let us recall that the LCP has a unique solution for all $\mathbf{a}$ if the matrix $\mathbf{W}$ is a positive definite matrix (Cottle *et al.*, 1992). It is

straightforward to identify the vector $\mathbf{a}$ in Eq. (32) as $\mathbf{a} = \mathbf{S}_{\bar{c}} \mathbf{w}_{\text{free}}^{n+1} + \varrho \boldsymbol{v}_{\bar{c}}^n$ and the matrix $\mathbf{W} = \mathbf{W}_{\bar{c}\bar{c}}$. In our application, the Delassus matrix $\mathbf{W}$ is obviously symmetric positive definite and a unique solution is ensured. If the string vibrates against a single point obstacle, the Delassus matrix reduces to a positive scalar and the LCP can be solved directly as

$$p_{\bar{c}}^{n+1} = \max\left(0, -\frac{1}{W_{\bar{c}\bar{c}}}\left(v_{\bar{c},\text{free}}^{n+1} + \varrho v_{\bar{c}}^n\right)\right). \qquad (33)$$

In the case of a distributed obstacle, a LCP solver has to be employed. In this article, we employ the numerical solvers provided by the SICONOS software (Acary *et al.*, 2016) which is dedicated to the modelling and simulation of nonsmooth dynamical systems. In SICONOS, several numerical algorithms are implemented to solve LCPs. Depending on the number of constraints and the required accuracy, pivoting, or projected successive overrelaxation (PSOR) techniques may be used (Cottle *et al.*, 1992). Simulations in the present paper are based on the use of a standard pivoting technique for solving LCP, known as Lemke's method (Cottle *et al.*, 1992) to get a high precision solution at the machine accuracy.

IV. NUMERICAL RESULTS

A. One contact point: The case of tanpura

In this section, the case of a two point bridge is considered, which consists in placing a point obstacle near a boundary. The string parameters are selected as in Issanchou *et al.* (2017) for the purpose of comparison. Geometric and material relevant properties are recalled in Table I. The point obstacle is located at 6 mm from the boundary $x = 0$, in agreement with the range of positions mentioned in Valette and Cuesta (1993) to mimic the tanpura bridge with a two point approximation.

The initial position of the string is a smoothed centered triangle with a maximal amplitude $u_{0,max} = 1.8$ mm and no velocity. The nonsmooth numerical procedure is compared to the power-law approach described in Issanchou *et al.* (2017), where the contact force is modeled as $f = K[\eta]_+^\alpha$, where $[\eta]_+ = \frac{1}{2}[\eta + |\eta|]$, with $K = 10^{13}$ and $\alpha = 1.5$ for simulations. In order to be in line with the assumptions retained in Issanchou *et al.* (2017), we select an equal number of modes N_m and grid points N, specifically $N_m = N - 1$, and set $N = 1002$ for the simulations. For completeness, the outcomes of the nonsmooth method are compared for both $\varrho = 0$ and $\varrho = 1$.

A convergence study has been led using the stringent criterion introduced in Issanchou *et al.* (2017) to control the long-term behaviour. The criterion inspects relative errors of the numerical results on a 3 s simulation and imposes the error to be less than 10^{-1}. Following that, the sampling frequency is selected as $F_s = 2$ MHz for both compliant and

TABLE I. Electric guitar string properties.

L (m)	d (mm)	T (N)	μ (kg m^{-1})
1.002	0.43	180.5	1.17×10^{-3}

B	δ_{ve}	Q_{te}^{-1}
1.78×10^{-5}	4.5×10^{-3}	2.03×10^{-4}

nonsmooth cases, since it has been found that the convergence is obtained at that sampling rate for the two methods.

The linear modal characteristics of the string are also selected as in Issanchou *et al.* (2017), eigenfrequencies and damping ratios resulting from an experimental identification on a real guitar string. The identification has been realised up to 7200 Hz, then models are employed to input linear characteristics into the simulation up to the desired maximal frequency. Models used for linear characteristics are recalled in the Appendix, and selected values resulting from model fitting shown in Issanchou *et al.* (2017) are given in Table II.

Figure 2 shows the string displacement at a point located at 1 cm from $x = L$. Associated sound files corresponding to the displacement resampled at 44.1 kHz are available as supplementary material.[1] Its appears that selecting $\varrho = 0$ or $\varrho = 1$ has no significant macroscopic effect on the simulation result. Both values give a temporal displacement extremely similar to that obtained with the penalty approach. In all cases, a crenel shape appears which evolves in time due to effects of dispersion and damping. As analysed for the power-law approach in Issanchou *et al.* (2017), where simulation outcomes are compared to experimental signals, we can thus conclude that the nonsmooth method also retrieves the essential features of the string vibration against a point obstacle, with the same global accuracy as that obtained with the penalty approach.

Spectrograms of numerical signals with the penalty approach and the nonsmooth method with $\varrho = 1$ are shown in Fig. 3. No significant difference is observed when $\varrho = 0$, therefore we do not show the spectrogram in this case. In both cases, there are no missing modes despite the centered initial condition, due to energy transfers induced by collisions. Moreover, both methods accurately recover the descending formant observed experimentally. Such formants constitute a distinctive feature of musical instruments such as tanpuras.

We now explore the local behaviour of the simulated string displacement at the obstacle position u_c in Fig. 4,

with the nonsmooth method, $\varrho = 0$ and $\varrho = 1$, as well as with the penalty approach. Zooms focus on the first two contact periods. Despite similar global waveshapes, the string has local specific and distinguishable behaviours, around the obstacle, when colliding with it. When $\varrho = 0$, as expected since no back velocity is enforced, the string sticks to the obstacle for a short period of time when colliding, and then leaves it when the wave propagates back (i.e., around 3.8×10^{-3} s for the first contact time, then around 8.8×10^{-3} s for the second contact). When $\varrho = 1$, the string bounces off the obstacle with a magnitude of about 10^{-7} m and the signal takes the form of one time step oscillations until the string leaves the obstacle for a longer time around 3.8×10^{-3} s. With the penalty approach, smoother oscillations appear with similar amplitudes. Interestingly, the envelope of oscillations of the nonsmooth signal closely fits oscillations of the compliant signal. The detailed behaviour of the string, computed with the nonsmooth method and different values of F_s, is presented in Fig. 5. Increasing the sampling frequency does not significantly change the global string behaviour, however, the local behaviour at the obstacle position is affected. Note also that a very small penetration occurs with the nonsmooth method, a numerical artifact linked to the time discretisation. This numerical penetration is reduced, and small bounces can be observed when $\varrho = 1$, after the string reaches the obstacle. When $\varrho = 0$, the string sticks to the obstacle at the height given by the first discrete point where contact condition is activated, defining the depth of this numerical penetration.

Finally, nonsmooth and power-law approaches give very similar results in the case of a point obstacle, and no significant difference is observed between simulations with $\varrho = 0$ and $\varrho = 1$ in the nonsmooth case, except when focusing on the obstacle position. This can be related to the analytic solutions for a string with a single contact point where a sticking time is obtained as long as the wave has not come back (see, e.g., Cabannes, 1984, 1987, Doyen *et al.*, 2011, and Yoong *et al.*, 2017 for similar cases with bars).

We now discuss time costs of the nonsmooth ($\varrho = 1$) and power-law ($\alpha = 1.5$, $K = 10^{13}$) approaches. Computation costs, excluding initialisation, saving data and energy computation, are presented in Table III. For the compliant method, they are presented either with a spatial grid which is fully
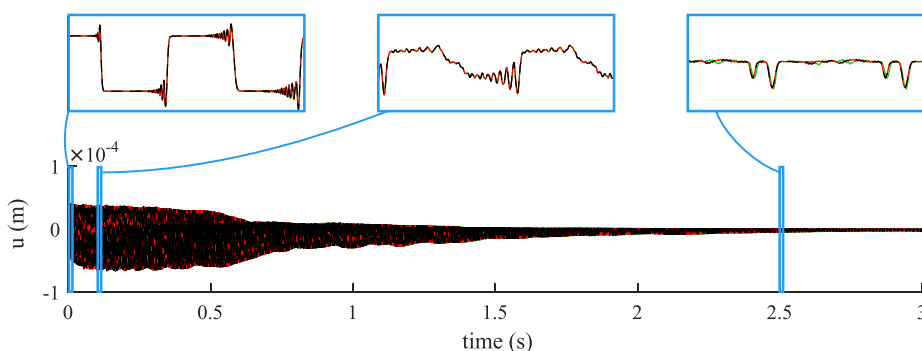

FIG. 2. (Color online) Displacement of the string vibrating against a point obstacle near a boundary, taken at 1 cm from the extremity $x = L$. Comparison between the penalty approach, $F_s = 2$ MHz (green line), and the nonsmooth method, $F_s = 2$ MHz, $\varrho = 0$ (black dashed line) and $\varrho = 1$ (red line).
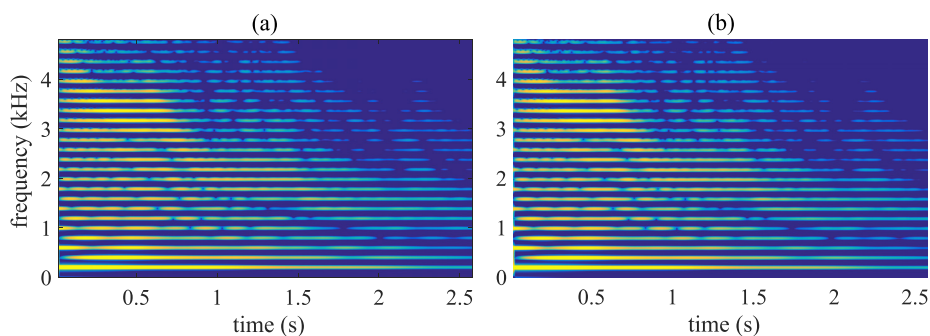
(a)   (b)

FIG. 3. (Color online) Spectrograms of the string displacement in the case of a point obstacle near a boundary (dB, with a 70 dB dynamic). (a) Power-law method, $F_s = 2\,\text{MHz}$. (b) Nonsmooth method, $F_s = 2\,\text{MHz}$, $\varrho = 1$.

included in the matrix **S**, meaning that its dimensions are $(N-1)^2$, or with a matrix S which only includes the obstacle position, meaning that its dimensions are $1 \times N - 1$. The former case strictly corresponds to the scheme presented in Issanchou *et al.* (2017), while the latter case (modified compliant method) contains an improvement where the number of grid points N is no longer related to the number of modes N_m. This further step is described in van Walstijn and Bridges (2016), and is also implemented for the nonsmooth method. All computations presented in Table III were led with MATLAB on a single CPU with a clock at 2.4 GHz.

One can observe that taking into account only the contact point in the modified compliant method allows one to obtain a significant gain in computational times since a factor of 2 is present as compared to the power-law method with a full **S** matrix. A more significant gain can be obtained due to the nonsmooth method: computation costs are 12 to 37 times smaller. This is due, in particular, to the reduced number of matrix vector products as well as a reduced time for solving the LCP (straightforward in the point obstacle case) compared to Newton-Raphson iterations. Note also that computation times has been found to be once again divided by a factor of 2 by running the same code with the

SICONOS software in a optimized C/C++ implementation (Acary *et al.*, 2016).

In this section, we discussed the behaviour of a string vibrating against a point obstacle, mimicking the case of a tanpura. We observed that the nonsmooth simulation in the case of a two point bridge was very close to the simulation led with the power-law method, both being consistent with experimental data presented in Issanchou *et al.* (2017). Moreover, it seems that the global behaviour of the string does not rely on the coefficient of restitution, even though the local string behaviour at the contact point does. In the following, we investigate a case implying multiple contact points.

B. Multiple contact points: Application to the electric bass

In this section, the complexity is increased by considering a string vibrating against the fretboard of an electric bass with up to 20 contact points. Electric basses are known for their modern playing techniques such as pop and slap where numerous contacts are intentionally provoked in the transient attack, giving a peculiar bright and percussive sound (Bacon, 2013; Issanchou *et al.*, 2018).
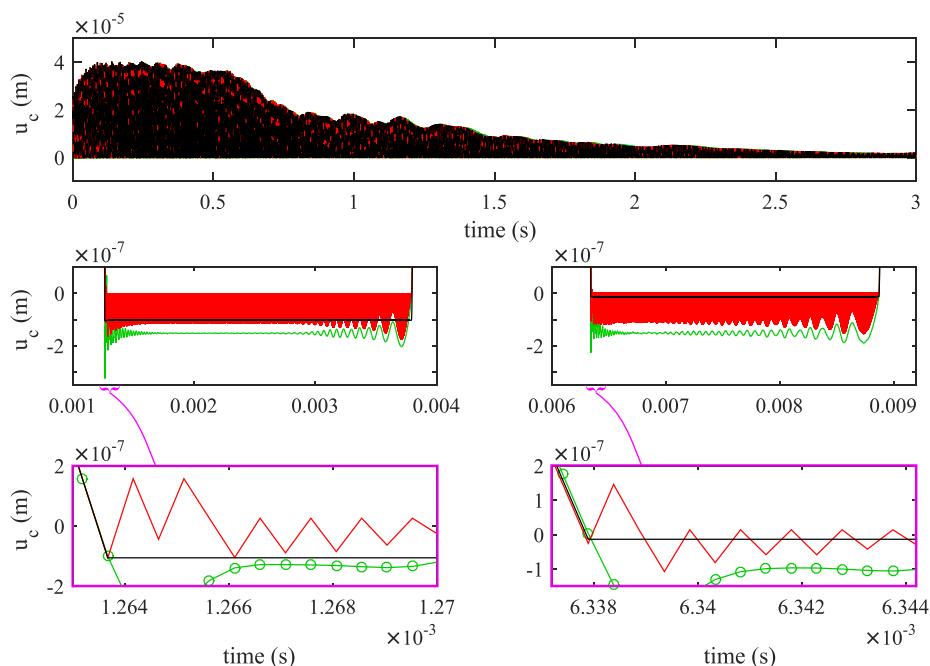

FIG. 4. (Color online) Displacement of the string vibrating at the obstacle position. Comparison between the numerical simulation with the penalty approach, $F_s = 2\,\text{MHz}$ (green line) and the nonsmooth method with $\varrho = 0$ (black dashed line, black line in zooms) and $\varrho = 1$ (red line), $F_s = 2\,\text{MHz}$.
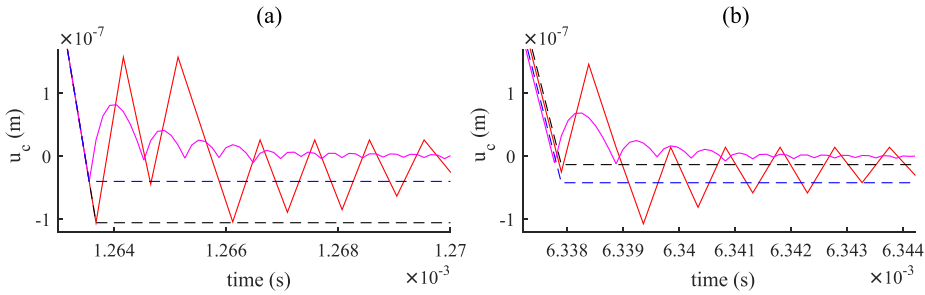
(a)

(b)

FIG. 5. (Color online) Displacement of the string at the obstacle position. Comparison between the numerical nonsmooth simulation with $F_s = 2$ MHz ($\varrho = 0$: black dashed line, $\varrho = 1$: red line) and $F_s = 8$ MHz ($\varrho = 0$: blue dashed line, $\varrho = 1$: magenta line). (a) First overall string/obstacle contact, (b) second overall string/obstacle contact.

Figure 6 shows the guitar neck profile with its 20 frets together with the initial condition imposed to the string. A G-string of an electric bass is considered for simulations, its properties are given in Table IV. The string is plucked at 64 cm from the nut with a maximal initial amplitude $u_{0,max} = 3.6$ mm. As in Sec. IV A and according to the study led in Issanchou et al. (2018), measured values of the linear characteristics are selected to fit with the model up to about 3400 Hz, then models are employed with parameters reported in Table V. In order to perform comparisons with the power-law approach and with experimental results obtained in Issanchou et al. (2018), 863 modes are retained for simulations. The convergence of data is determined according the criterion presented in Issanchou et al. (2017); Issanchou et al. (2018) applied over a period of time recovering all string/neck collisions. This implies large values of F_s, nevertheless smaller values may be selected for other applications. For instance, a convergence study on the spectral content, associated to a perception evaluation of signals with different F_s, may lead to smaller values of F_s with a satisfactory sound rendition. This is, however, not the purpose of the present paper.

Temporal results are shown in Fig. 7, with a comparison of the nonsmooth approach with the experimental result already shown in Issanchou et al. (2018), and then with the compliant method. A spectral comparison is provided due to the spectrograms of the displacements shown in Fig. 8. Related sound files corresponding to the displacement resampled at 44.1 kHz are available as supplementary material.[1] The presence of multiple contacts makes the dynamics more complex but leads once again to similar results for the two limit values of the restitution coefficient, namely, $\varrho = 0$ and $\varrho = 1$. Simulation results show that the temporal signals are almost coincident. Consequently, only the case $\varrho = 1$ is presented. It thus appears that the dynamics of collisions, from a macroscopic point of view, is still dominated by waves going back and forth in inter-fret intervals.

Comparing outcomes of the displacement obtained with the nonsmooth method with experimental results shows an excellent agreement, both in the global shape of the time series and in the details shown in zooms in Fig. 7. The occurrence of a substantial high frequency content from the very first collisions is clearly ascertained and retrieved, and the long term behaviour remains similar. A few discrepancies appear, however, as explained in Issanchou et al. (2018) they are probably mainly due to (i) uncertainties related to the experimental measurement of the neck profile and, to a lesser extent, to the measured properties of the string; (ii) the assumption that the fretboard is a rigid obstacle. Comparing the two numerical methods shows that they behave very similarly, with only slight discrepancies.

Focusing on spectrograms, a similar structure between experimental and numerical data can be observed. In particular, energy transfers appear in the transient attack between 0 and 0.09 s, this time window corresponding to the occurrence of contacts between the string and the fretboard. Once again, this collision period of time, together with specific reinforced spectral zones (e.g., around 4500 Hz), is particularly well retrieved by numerical simulations. From a perceptive point of view, associated sounds, given as supplementary material,[1] are very close to the ear.

Finally, the global dynamics of the string colliding with frets is well described by both compliant and nonsmooth

TABLE III. Computation times with the compliant and nonsmooth methods (implemented in MATLAB), in seconds, for the simulation of a one second signal in the case of a point obstacle.

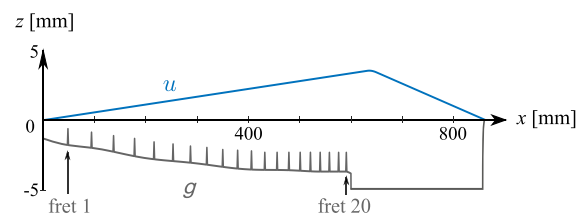| Compliant approach, full spatial grid included in S				
F_s (kHz)	44.1	88.2	176	1000
Newton-Raphson	30	55	105	362
Other operations	175	352	710	3964
Total time	205	407	815	4326
Compliant approach, S at the obstacle position only				
F_s (kHz)	44.1	88.2	176	1000
Newton-Raphson	7.7	12	29	140
Other operations	100	196	343	1592
Total time	108	208	372	1732
Nonsmooth method				
F_s (kHz)	44.1	88.2	176	1000
LCP	1.4	5.3	3.9	21
Computation in Eq. (27)	1.4	2.6	5.2	38
Other operations	4.3	8.0	13	83
Total time	7.1	16	22	142

FIG. 6. (Color online) A string vibrating against a bass guitar fretboard represented by the function g.

TABLE IV. Electric bass string properties.

L (m)	d (mm)	d_{core} (mm)	T (N)	μ (kg m^{-1})
0.863	1.14	0.43	191.6	6.69×10^{-3}

TABLE V. Models parameters for the electric bass string installed on an electric bass.

B	δ_{ve}	Q_{te}^{-1}
3.5×10^{-5}	0.01	6×10^{-6}

approaches. In the studied configuration, both numerical methods produce very similar results at the measurement point considered, selected from experiments. Furthermore, the value of the restitution coefficient ϱ does not substantially affect simulations, meaning that, in the present case, the nonsmooth approach would be free of parameters to be adjusted.

The simulation of 0.1 s of signal (time interval recovering all contacts) at $F_s = 1$ MHz lasts 5 min with MATLAB while it lasts only 30 s with SICONOS. Numerical costs are thus found to be divided by a factor 10: once again, an important gain in computation can be achieved with the nonsmooth method on SICONOS.

V. CONCLUSION

A nonsmooth approach to the numerical simulation of musical strings colliding with an obstacle has been presented. The main feature consists in combining an exact scheme for the vibratory (linear) part and a Moreau-Jean scheme for the contact force, embedded in a modal description of the dynamics. This results in a computationally efficient scheme preventing numerical dispersion during free flight phases. The method has been tested on two cases involving either one contact point (a two point bridge mimicking a tanpura) or multiple contacts (the case of an electric bass). In both cases, it has been found that the nonsmooth approach is very accurate and compares well with experiments and simulations led with a compliant method. A significant gain in computational times is obtained with the proposed nonsmooth method. Interestingly, for the two test cases, simulation results are relatively insensitive to the choice of the value of the restitution coefficient, so that the model could finally be considered as free of parameters to describe collisions. This particular behaviour should, however, be limited to a few number of pointwise contacts where, from a macroscopic point of view, the behaviour during collisions is governed by waves going back and forth in the string. In contrast, the coefficient of restitution should have an effect when considering a large number of contact points or continuous contact regions (e.g., a fretless bass), where sticking may occur on a whole interval. Note also that the nonsmooth method has been tested in specific examples where a hard collision is at hand and no specific physical detail on the contact is needed to have efficient simulations accounting for the rich contact dynamics of the string. For other cases encountered in musical acoustics where the contact is softer, e.g., mallet/membrane or finger/string interactions, the nonsmooth approach may also be used, either with a refined continuous description of the deformable bodies, involving an increase of the computational burden to take into account the whole dynamics; or with a localised behaviour law to account for the felt as done, for example, in Thorin et al. (2017). These points are thus left for further studies where a more complete comparison of nonsmooth and compliant methods could be given.
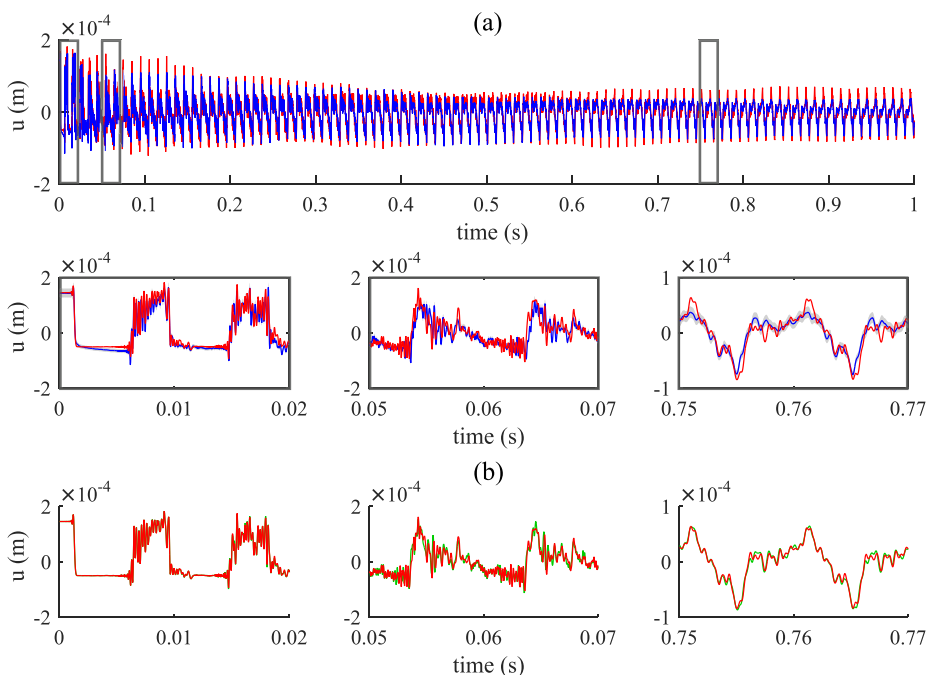

FIG. 7. (Color online) Displacement of the string vibrating against the neck of a bass guitar, taken at 9 mm from the extremity $x = L$. Comparison between the experimental signal (blue line) and the nonsmooth method, $\varrho = 1$, $F_s = 4$ MHz (red line), and between the nonsmooth method, $\varrho = 1$, $F_s = 4$ MHz (red line) and the compliant method, $F_s = 8$ MHz (green line).

J. Acoust. Soc. Am. **143** (5), May 2018
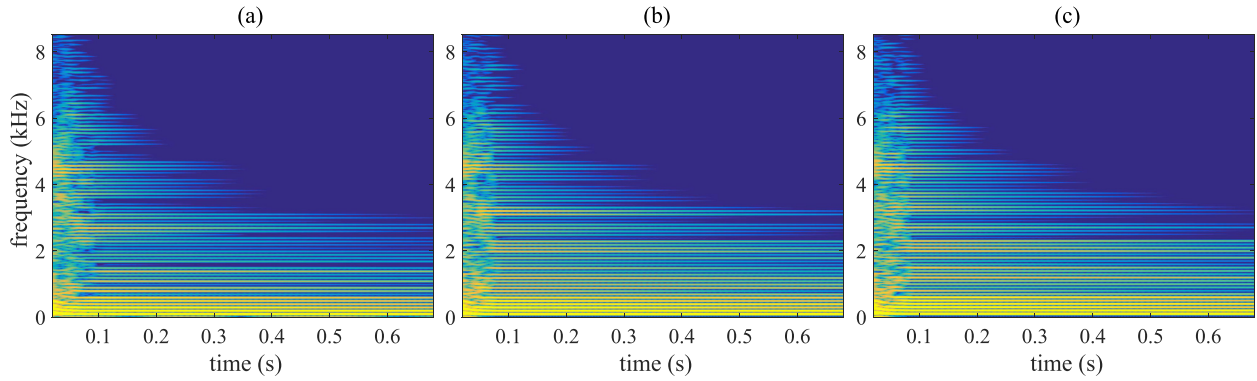
Issanchou et al.   3203

FIG. 8. (Color online) Spectrograms of the string displacement on an electric bass (dB, with a 70 dB dynamic). (a) Experimental signal, (b) compliant method, $F_s = 8\,\text{MHz}$, (c) nonsmooth method, $F_s = 4\,\text{MHz}$, $\varrho = 1$.

APPENDIX: LINEAR CHARACTERISTICS

A complete model for the computation of eigenfrequencies is given in Issanchou *et al.* (2018) which includes the tension and the stiffness of the string, together with the potential mobility at one extremity, as observed, e.g., for string instruments such as bass and guitar. The eigenfrequencies are then described by

$$\nu_j = j\frac{c}{2L}\left(1 + \frac{Bj^2}{2} + \frac{\mu c}{j\pi}\,\text{Im}\left(Y_{nut}(\omega_{0,j})\right)\right), \tag{A1}$$

where $c = \sqrt{T/\mu}$ is the wave velocity of the ideal string, $B = \pi^2 EI/TL^2$ is the inharmonicity coefficient, and Y_{nut} is the mobility at the nut, evaluated at $\omega_{0,j} = j(\pi c/L)$. In this paper, the mobility is taken as zero in the case of a two point bridge while it takes measured values [see Issanchou *et al.* (2018)] in the case of an electric bass.

Damping parameters are modeled through the quality factor $Q_j = \pi\nu_j/\sigma_j$, such that

$$Q_j^{-1} = Q_{j,\text{air}}^{-1} + Q_{j,\text{ve}}^{-1} + Q_{\text{te}}^{-1} + \frac{\mu c^2}{\pi L\nu_j}\,\text{Re}\left(Y_{nut}(\omega_j)\right), \tag{A2}$$

where subscripts air, ve, and te, respectively, refer to losses due to air friction, viscoelastic effects, and thermoelastic effects. Their detailed expressions are given by

$$Q_{j,\text{air}}^{-1} = \frac{jc}{2L\nu_j}\frac{R}{2\pi\mu\nu_j}, \tag{A3}$$

$$Q_{j,\text{ve}}^{-1} = \frac{4\pi^2\mu E_{core}I_{core}\delta_{\text{ve}}}{T^2}\frac{\nu_{0,j}^3}{\nu_j}, \tag{A4}$$

where $R = 2\pi\eta_{\text{air}} + 2\pi d_{eq}\sqrt{\pi\eta_{\text{air}}\rho_{\text{air}}\nu_j}$, with η_{air} and ρ_{air} the dynamic viscosity coefficient and the air density, respectively. Usual values $\eta_{\text{air}} = 1.8 \times 10^{-5}\,\text{kg}\,\text{m}^{-1}\,\text{s}^{-1}$ and $\rho_{\text{air}} = 1.2\,\text{kg}\,\text{m}^{-3}$ are selected. The employed equivalent diameter is expressed as

$$d_{eq} = \frac{\pi}{2}\left(\left(1 + \frac{2}{\pi}\right)2r_{winding} + 2r_{core}\right), \tag{A5}$$

where $r_{winding}$ and r_{core} are the radii of the string winding and core, respectively. Viscoelastic effects are assumed to be located in the string core so that the Young's modulus E_{core}

and the moment of inertia $I = \pi r_{core}^4/4$ are related to the core only. The notation $\nu_{0,j}$ refers to the value $jc/2L$ and Q_{te}^{-1} is taken as a constant.

Acary, V. (**2016**). "Energy conservation and dissipation properties of time-integration methods for nonsmooth elastodynamics with contact," ZAMM **96**(5), 585–603.

Acary, V., Brémond, M., Huber, O., and Pérignon, F. (**2016**). "Siconos. A software for modeling and simulation of nonsmooth dynamical systems," http://siconos.gforge.inria.fr (Last viewed May 20, 2018).

Acary, V., and Brogliato, B. (**2008**). "Numerical methods for nonsmooth dynamical systems. Applications in mechanics and electronics," Vol. 35 of Lecture Notes in Applied and Computational Mechanics (Springer Verlag, Berlin).

Acary, V., de Jong, H., and Brogliato, B. (**2014**). "Numerical simulation of piecewise-linear models of gene regulatory networks using complementarity systems," Physica D **269**, 103–119.

Ahn, J. (**2007**). "A vibrating string with dynamic frictionless impact," Appl. Numer. Math. **57**, 861–884.

Amerio, L. (**1978**). "Continuous solutions of the problem of a string vibrating against an obstacle," Rend. Semin. Matemat. Univ. Padova **59**, 67–96.

Bacon, T. (**2013**). "Electric bass guitar," in *Grove Music Online, Oxford Music Online* (Oxford University Press, Oxford), https://doi.org/10.1093/gmo/9781561592630.article.45729 (Last viewed May 20, 2018).

Bertails-Descoubes, F., Cadoux, F., Davier, G., and Acary, V. (**2011**). "A nonsmooth Newton solver for capturing exact Coulomb friction in fiber assemblies," ACM Trans. Graph. **30**(1), 6.

Bilbao, S. (**2009**). *Numerical Sound Synthesis: Finite Difference Schemes and Simulation in Musical Acoustics* (Wiley, Chichester).

Bilbao, S. (**2012**). "Time domain simulation of the snare drum," J. Acoust. Soc. Am. **131**, 914–925.

Bilbao, S., and Torin, A. (**2015**). "Numerical modeling and sound synthesis for articulated string/fretboard interaction," J. Audio Eng. Soc **63**, 336–347.

Bilbao, S., Torin, A., and Chatziioannou, V. (**2015**). "Numerical modeling of collisions in musical instruments," Acta Acust. united Acust. **101**, 155–173.

Boutillon, X. (**1988**). "Model for piano hammers: Experimental determination and digital simulation," J. Acoust. Soc. Am. **83**, 746–754.

Cabannes, H. (**1984**). "Periodic motions of a string vibrating against a fixed point-mass obstacle: II," Math. Meth. Appl. Sci. **6**, 55–67.

Cabannes, H. (**1987**). "Motion of a string vibrating against a rigid fixed obstacle," Math. Modell. **8**, 364–365.

Chatziioannou, V., and van Walstijn, M. (**2015**). "Energy conserving schemes for the simulation of musical instrument contact dynamics," J. Sound Vib. **339**, 262–279.

Chen, Q.-Z., Acary, V., Virlez, G., and Brüls, O. (**2013**). "A nonsmooth generalized-α scheme for flexible multibody systems with unilateral constraints," Int. J. Numer. Meth. Eng. **96**(8), 487–511.

Citrini, C. (**1991**). "Vibrating strings with obstacles: The analytic study," in *Advances in Kinetic Theory and Continuum Mechanics*, edited by G. R. Soubbaramayer (Springer, Berlin), pp. 249–259.

Cottle, R. W., Pang, J., and Stone, R. E. (**1992**). *The Linear Complementarity Problem* (Academic Press, Boston, MA).

Desvages, C., and Bilbao, S. (**2015**). "Two-polarisation finite difference model of bowed strings with nonlinear contact and friction forces," in *International Conference on Digital Audio Effects, DAFx-15*, Trondheim.

Doyen, D., Ern, A., and Piperno, S. (**2011**). "Time-integration schemes for the finite element dynamic Signorini problem," *SIAM J. Sci. Comput.* **33**(1), 223–249.

Ducceschi, M., Bilbao, S., and Desvages, C. (**2016**). "Modelling collisions of nonlinear strings against rigid barriers: Conservative finite difference schemes with application to sound synthesis," in *International Congress on Acoustics ICA*, Buenos Aires.

Fletcher, N. H., and Rossing, T. D. (**1998**). *The Physics of Musical Instruments*, 2nd ed. (Springer, New York).

Goldsmith, W. (**2001**). *Impact* (Dover, Mineola).

Inácio, O., Henrique, L., and Antunes, J. (**2006**). "The dynamics of Tibetan singing bowls," Acta Acust. Acust. **92**(4), 637–653.

Issanchou, C., Bilbao, S., Le Carrou, J.-L., Touzé, C., and Doaré, O. (**2017**). "A modal-based approach to the nonlinear vibration of strings against a unilateral obstacle: Simulations and experiments in the pointwise case," *J. Sound Vib.* **393**, 229–251.

Issanchou, C., Le Carrou, J.-L., Touzé, C., Fabre, B., and Doaré, O. (**2018**). "String/frets contacts in the electric bass sound: Simulations and experiments," *Appl. Acoust.* **129**, 217–228.

Janin, O., and Lamarque, C.-H. (**2001**). "Comparison of several numerical methods for mechanical systems with impacts," *Int. J. Numer. Meth. Eng.* **51**, 1101–1132.

Jean, M. (**1995**). "Frictional contact in collections of rigid or deformable bodies: Numerical simulation of geomaterial motions," in *Mechanics of Geomaterial Interfaces*, edited by A. Selvadurai and M. Boulon, Vol. 42 of Studies in Applied Mechanics (Elsevier, Amsterdam), pp. 463–486.

Jean, M. (**1999**). "The non-smooth contact dynamics method," *Comput. Meth. Appl. Mech. Eng.* **177**(3), 235–257.

Jean, M., and Moreau, J.-J. (**1987**). *Dynamics in the Presence of Unilateral Contacts and Dry Friction: A Numerical Approach* (Springer Vienna, Vienna), pp. 151–196.

Mandal, A. K., and Wahi, P. (**2015**). "Natural frequencies, modeshapes and modal interactions for strings vibrating against an obstacle: Relevance to Sitar and Veena," *J. Sound Vib.* **338**, 42–59.

Meingast, M. B., Legrand, M., and Pierre, C. (**2014**). "A linear complementarity problem formulation for periodic solutions to unilateral contact problems," *Int. J. Non-Linear Mech.* **66**, 18–27.

Moreau, J. (**1988**). "Bounded variation in time," in *Topics in Nonsmooth Mechanics*, edited by J. Moreau, P. Panagiotopoulos, and G. Strang (Birkhäuser, Basel), pp. 1–74.

Moreau, J. (**1999**). "Numerical aspects of the sweeping process," *Comput. Meth. Appl. Mech. Eng.* **177**, 329–349.

Nguyen, N. S., and Brogliato, B. (**2014**). *Multiple Impacts in Dissipative Granular Chains*, Vol. 72 of Lecture Notes in Applied and Computational Mechanics (Springer Verlag, Berlin).

Paoli, L., and Schatzman, M. (**2002**). "A numerical scheme for impact problems. I: The one-dimensional case," *SIAM J. Numer. Anal.* **40**(2), 702–733.

Paté, A., Le Carrou, J.-L., and Fabre, B. (**2014**). "Predicting the decay time of solid body electric guitar tones," *J. Acoust. Soc. Am.* **135**(5), 3045–3055.

Raman, C. (**1921**). "On some Indian stringed instruments," Indian Assoc. Cultivat. Sci. **7**, 29–33.

Renouf, M., Dubois, F., and Alart, P. (**2004**). "A parallel version of the non smooth contact dynamics algorithm applied to the simulation of granular media," *J. Comput. Appl. Math.* **168**(1), 375–382.

Rhaouti, L., Chaigne, A., and Joly, P. (**1999**). "Time-domain modeling and numerical simulation of a kettledrum," *J. Acoust. Soc. Am.* **105**(6), 3545–3562.

Schatzman, M. (**1980**). "A hyperbolic problem of second order with unilateral constraints: The vibrating string with a concave obstacle," *J. Math. Anal. Appl.* **73**, 138–191.

Siddiq, S. (**2012**). "A physical model of the nonlinear sitar string," *Arch. Acoust.* **37**(1), 73–79.

Signorini, A. (**1933**). "Sopra alcune questioni di statica dei sistemi continui" ("Above some static issues of continuous systems"), Ann. Scuola Norm. Super. Pisa **2**, 231–251.

Studer, C. (**2009**). *Numerics of Unilateral Contacts and Friction*, Vol. 47 of Lecture Notes in Applied and Computational Mechanics (Springer Verlag, Berlin).

Thorin, A., Boutillon, X., Lozada, J., and Merlhiot, X. (**2017**). "Non-smooth dynamics for an efficient simulation of the grand piano action," *Meccanica* **52**(11-12), 2837–2854.

Trautmann, L., and Rabenstein, R. (**2004**). "Multirate simulations of string vibrations including nonlinear fret-string interactions using the functional transformation method," *EURASIP J. Adv. Sign. Process.* **7**, 949–963.

Valette, C., and Cuesta, C. (**1993**). *Mécanique de la Corde Vibrante* (*Mechanics of the Vibrating Rope*) (Hermès, Paris).

Valette, C., Cuesta, C., Besnainou, C., and Castellengo, M. (**1991**). "The tanpura bridge as a precursive wave generator," Acustica **74**, 201–208.

van Walstijn, M., and Bridges, J. (**2016**). "Simulation of distributed contact in string instruments: A modal expansion approach," in *European Signal Processing Conference (EUSIPCO)*, pp. 1023–1027.

van Walstijn, M., Bridges, J., and Mehes, S. (**2016**). "A real-time synthesis oriented tanpura model," in *International Conference on Digital Audio Effects, DAFx-16*, Brno.

Vyasarayani, C. P., Birkett, S., and McPhee, J. (**2009**). "Modeling the dynamics of a vibrating string with a finite distributed unilateral constraint: Application to the sitar," *J. Acoust. Soc. Am.* **125**(6), 3673–3682.

Yoong, C., Thorin, A., and Legrand, M. (**2017**). "Nonsmooth modal analysis of an elastic bar subject to a unilateral contact constraint," *Nonlin. Dyn.* **91**, 2453–2476.